Temperature and doping-level dependence of magnetic order in $La_{2-x}Sr_xNiO_{4+\delta}$ studied by muon spin rotation

Th. Jestädt,* K. H. Chow,† S. J. Blundell, W. Hayes, F. L. Pratt, and B. W. Lovett
Clarendon Laboratory, University of Oxford, Parks Road, Oxford, OX1 3PU, United Kingdom

M. A. Green, J. E. Millburn, and M. J. Rosseinsky
Inorganic Chemistry Laboratory, University of Oxford, South Parks Road, Oxford, OX1 3QR, United Kingdom
(Received 29 June 1998; revised manuscript received 15 October 1998)

We report muon-spin-rotation (μSR) measurements on a series of compounds with composition $La_{2-x}Sr_xNiO_{4+\delta}$ with strontium doping level x between 0 and 1. A magnetic transition is found in all the samples studied, which occurs at a composition-dependent temperature, T_M. Below T_M clear precession signals are observed in zero applied magnetic field for all x, indicating the existence of at least short-range magnetic order on a time scale longer than 10^{-8} s. Above T_M the magnetic correlation times decrease by several orders of magnitude. At $x \approx 0.33$, we find peaks in both T_M and the zero-temperature staggered magnetization, an observation which we attribute to the higher degree of localization of the holes at this doping level. The measurements of T_M as a function of x extend the determination of Néel temperatures by previous neutron diffraction and μSR measurements. [S0163-1829(99)09505-3]

I. INTRODUCTION

La_2NiO_4 and La_2CuO_4 are antiferromagnetic insulators with the layered perovskite (K_2NiF_4) structure; they have a high degree of oxygen $2p$ character in the valence band and transition metal $3d$ character in the conduction band. Hole doping can be achieved by (1) substitution of Sr^{2+} for La^{3+} or (2) intercalation of excess oxygen. Although $La_{2-x}Sr_xCuO_{4+\delta}$ and $La_{2-x}Sr_xNiO_{4+\delta}$ are isostructural (though with different tilting distortions), there are dramatic differences in the effects of hole doping on their electrical and magnetic properties. In $La_{2-x}Sr_xCuO_{4+\delta}$ antiferromagnetic long-range order is replaced by short-range two-dimensional (2D) correlations for $x \geqslant 0.02$ (Refs. 1 and 2) and the material becomes metallic and superconducting with the maximum T_C at $x \sim 0.15$.[3] $La_{2-x}Sr_xNiO_{4+\delta}$ shows significant enhancement in conductivity (seen beyond $x=0.6$), with truly metallic behavior down to $T=5$ K beyond $x \sim 1$, but no superconductivity is observed at any composition.[4,5]

The differences between $La_{2-x}Sr_xCuO_{4+\delta}$ and $La_{2-x}Sr_xNiO_{4+\delta}$ provide an incentive to understand the nature of the ground state in the doped nickelates and consequently their magnetic properties have been investigated using a variety of methods. Electron diffraction[6] and neutron scattering[7–12] measurements have been instrumental in providing detailed microscopic information on the arrangement of the spins and holes in lightly doped nickelates. Electron diffraction studies[6] find evidence for a 2D ordered array of localized doped holes at low temperatures for $x<0.5$. The spin as well as the charge structures have also been probed extensively by neutron diffraction measurements.[7–16] These studies in general agree that as the doping level of the holes in the nickelates is increased, 3D antiferromagnetic order is suppressed and is replaced by 2D incommensurate correlations within the Ni-O planes. In particular, many interesting measurements have been reported for samples with no strontium, i.e., $x=0, \delta \neq 0$. For example, Refs. 9 and 11 report an ordering of interstitial oxygens for $\delta = 0.125$ near room temperature and provide convincing evidence that below 110 K the magnetic state consists of antiferromagnetic stripes of nickel spins separated by periodically spaced antiphase domain walls to which the holes segregate. In $La_2NiO_{4+\delta}$ magnetic order remains commensurate for $0<\delta<0.11$, although there is a pronounced variation of the magnetic transition temperature (T_M) with δ. Whereas a large number of articles have been published on the properties of $La_2NiO_{4+\delta}$ and $La_{2-x}Sr_xNiO_{4+\delta}$ with $x=0.33$, less is known about the properties of the strontium doped materials for $x \neq 0.33$, especially for large x. Anomalies in the magnetic susceptibility and resistivity have been reported[5,6,17] for $x=\frac{1}{3}$ and $\frac{1}{2}$. Hole ordering in the Ni-O planes, perhaps enhanced by commensurability effects at these magic numbers,[6,13,17] are believed to be responsible for this behavior. Furthermore, a recent neutron scattering study[18] of $La_{1.67}Sr_{0.33}NiO_4$ suggests that charge ordering is the driving force for magnetic ordering in this material.

In this paper we significantly extend earlier muon-spin-rotation (μSR) studies[19] of the magnetism of $La_{2-x}Sr_xNiO_{4+\delta}$ to cover the range $0.00<x<1.00$, allowing us to answer questions about the magnetic phase diagram and the appropriate parameter for the characterization of the magnetic to nonmagnetic transition. The μSR technique,[20] by virtue of the sizeable magnetic moment of the muon (spin 1/2, gyromagnetic ratio $\gamma_\mu = 2\pi \times 1.3554 \times 10^8$ Hz/T), is a sensitive method for investigating *local* magnetic order in solids and spin fluctuation rates in the range 10^4–10^{12} s^{-1}. Our measurements complement other investigations of the nickelates by (1) providing information on the temperature and composition dependence of the magnetic short-range order parameter, (2) enabling estimates of the magnetic transition temperatures T_M and the corresponding phase diagram to be made, and (3) making estimates of the spin fluctuation rates.

TABLE I. Polycrystalline $La_{2-x}Sr_xNiO_{4+\delta}$ samples studied and magnetic transition temperatures T_M obtained from μSR measurements.

x	δ	T_M(K)
0.00	0.009(4)[b]	335±5
0.15	0.01(1)	28±9
0.20	0.08(1)	133±14
0.20	0.052(3)[b]	125±9
0.25[a]	0.090	119±6
0.33[a]	0.09(1)	180±7
0.33	0.010(4)[b]	207±2
0.33	0.08(1)	204±9
0.40[a]	0.08(1)	118±13
0.40	0.06(1)	131±7
0.40	0.008(3)[b]	107±5
0.50[a]	0.065(3)[b]	73±10
0.50	0.006(4)	53±10
0.60[a]	0.095(4)[b]	67±5
0.60	0.01(1)	75±2
0.80	0.05(1)[b]	80±8
1.00[a]	0.063(4)[b]	44±14
1.00	0.02(1)	49±5
1.00	0.007(3)[b]	42±5

[a]Data from Ref. 19.

[b]Indicates determination of the oxygen content by thermogravimetric analysis (TGA) *and* iodometry (the oxygen content in the remaining samples were obtained using TGA only).

In particular, unambiguous evidence of a magnetic transition is found in all the samples studied. Below the transition temperature we observe muon precession signals in zero-applied field. This shows that there is at least short range magnetic order on a time scale longer than 10^{-8} s at low temperatures, indicating that speculations[21,22] that the strontium doped compounds might have a spin glass ground state for certain doping levels need reexamination (see Sec. IV). Above T_M the correlation time of the internal magnetic field at the muon decreases by several orders of magnitude. An interesting observation is that both T_M and the zero temperature staggered magnetization $M^{\dagger}(x,T=0\ \mathrm{K})$ show a peak at $x=0.33$, a fact that we believe is due to the enhanced hole localization at this strontium doping level.

The remainder of this article is arranged as follows. In Sec. II details of the sample preparation and characterization procedure are given. In Sec. III we give a short description of μSR techniques used in this study and in Sec. IV we present and discuss our results, stressing in particular the magnetic order in the samples, the dynamic and static nature of the Ni spins, and the phase diagram of the doped samples. In this section we also discuss the likely muon site(s) in our samples. Section V contains concluding remarks.

II. SAMPLE PREPARATION AND CHARACTERIZATION

Table I lists the nineteen polycrystalline $La_{2-x}Sr_xNiO_{4+\delta}$ samples that were investigated, including six samples on which earlier μSR measurements were done.[19] The samples studied were prepared as follows: stoichiometric quantities of $SrCO_3$, La_2O_3 (dried at 800 °C) and nickel powder were dissolved in 150 ml of dilute nitric acid. Citric acid and ethylene glycol were added and the mixture was heated, while stirring, to evaporate the solution. The resulting gel was decomposed at 350 °C overnight and the powder produced was refired at 800 °C in air, made into pellets and refired at temperatures between 1250 and 1450 °C in O_2 for an average of 10 days with several intermittent regrindings. Samples with a low oxygen doping were prepared by annealing in a N_2 atmosphere with 10% H_2 at ~300 °C for 6 h. The phase purity of all samples was confirmed using x-ray powder diffraction. The oxygen content of the samples was determined by thermogravimetric analysis under 8% H_2 in N_2. Some of the samples were also characterized by iodometry (see Table I).

III. EXPERIMENTAL ASPECTS

All the samples were measured using the μSR technique at the EMU and MuSR beamlines at ISIS (U.K.) to determine the temperature dependence of the initial decay asymmetry and the high-temperature relaxation rates (see below). In addition, selected samples were investigated at the πM3 and μE1 beamlines at PSI (Switzerland). It is important to note that PSI is a continuous-source muon facility while ISIS provides a pulsed beam of muons with a half width at half maximum of 70 ns. Because of the relatively low random background positron counts at a pulsed muon source, experiments at ISIS are able to measure data reliably to longer times (~16 μs) than at PSI (~7 μs). However, signals with precession frequencies and relaxation rates greater than ~5 MHz or 5 μs^{-1} are not resolvable at ISIS. In contrast, at PSI much higher frequencies and relaxation rates can be observed.

In a μSR experiment[20] a beam of nearly completely polarized positive muons (in most of our experiments with nominal momentum of 28 MeV/c) is stopped in a target sample. The muons (lifetime 2.2 μs) occupy an interstitial position in the crystal, typically within much less than one nanosecond. The observed quantity is the time evolution of the muon-spin polarization, which depends on the distribution of internal magnetic fields and their temporal fluctuations. Each muon decays into two neutrinos and a positron that is emitted preferentially along the instantaneous direction of the muon spin. Thus recording the time dependence of the positron emission directions gives direct information about the spin polarization of the ensemble of muons. The behavior of the polarization depends on the local magnetic field at the muon site and hence enables us to investigate short-range magnetic order in these materials.

In our experiments positrons are detected by scintillation counters placed forward and backward to the initial muon polarization direction. Histograms $N_F(t)$ and $N_B(t)$ record the number of positrons detected in the forward (F) and backward (B) detector as a function of time following the muon implantation. We have

$$P_z(t)=\frac{N_B(t)-\alpha N_F(t)}{N_B(t)+\alpha N_F(t)}, \tag{3.1}$$

where α is an experimental calibration constant which is usually close to unity. P_z is the spin polarization function [typically with $P_z(0)\approx 0.2$], and is the quantity of interest in a muon experiment.

If all the muons sense the same internal magnetic field $\mathbf{B}_\mu$, their moments will precess at the Larmor frequency $\omega_\mu = 2\pi\nu_\mu = \gamma_\mu B_\mu$ (provided that $\mathbf{B}_\mu$ is not parallel to the initial muon polarization). However, if the *direction* of the magnetic field is random but its magnitude is the same (such as in a polycrystalline sample), the muon-spin polarization function will be given by

$$P_z(t) = G_\parallel(t) + G_\perp(t)\cos(\omega_\mu t), \tag{3.2}$$

where $G_\perp(0)/G_\parallel(0) = 2$. The first term describes the polarization parallel to the local fields (zero-frequency component) while the second term describes the precession and relaxation of *transverse* components. In the absence of an external field, the frequency ω_μ is proportional to the internal magnetic field at the muon site and hence to the local magnetic order parameter, i.e. the staggered magnetization. The form of $G_\parallel(t)$ and $G_\perp(t)$ can also provide important information on whether the magnetic field at the muon site is static or dynamic. There are several cases which are relevant for the interpretation of our experimental results: (1) If the internal fields are static and their magnitudes take on a single value, $G_\parallel(t) = 1/3$ and $G_\perp(t) = 2/3$. (2) If the internal fields are static but there is a distribution in their values, $G_\parallel(t) = 1/3$ but $G_\perp(t)$ will be a relaxing function. (3) Finally, if the muon senses temporal fluctuations in the magnetic field, both $G_\parallel(t)$ and $G_\perp(t)$ will decay. In the majority of our experiments $P_z(t)$ was monitored with no external field applied, so it reflects the interaction of the implanted muon with the *internal* magnetic field. This is called zero field (ZF) μSR (the Earth's magnetic field was compensated to better than 10 μT). Longitudinal-field (LF) measurements, in which an external magnetic field is applied parallel to the initial muon polarization direction, were also made on some of the samples. In our experiments, polycrystalline samples of a typical mass of 2 g were packed in a silver foil (thickness 25 μm) pocket (typical dimensions are 20 mm $\times$17 mm $\times$2 mm) and mounted on a silver backing plate in the cryostat. Silver is used because it gives a nonrelaxing muon signal [and hence only contributes an added constant to $P_z(t)$].

IV. EXPERIMENTAL RESULTS AND DISCUSSION

In this section, we begin by describing the general features of the data. Then, in various subsections, we elaborate on particular aspects and discuss their physical relevance in more detail. There are two distinct temperature regimes in all the samples we have examined. In the ISIS experiments the following results were obtained: At temperatures above the magnetic transition temperature T_M, $P_z(t)$ is well described by a Gaussian function $Ae^{-\sigma^2 t^2}$. However, when $T < T_M$ there is a marked decrease in the apparent initial amplitude as well as a change in the line shape to a more exponential character. The decrease in the observed asymmetry is due to a fast-relaxing and/or a high-frequency component which cannot, as discussed in Sec. III, be resolved at ISIS. This

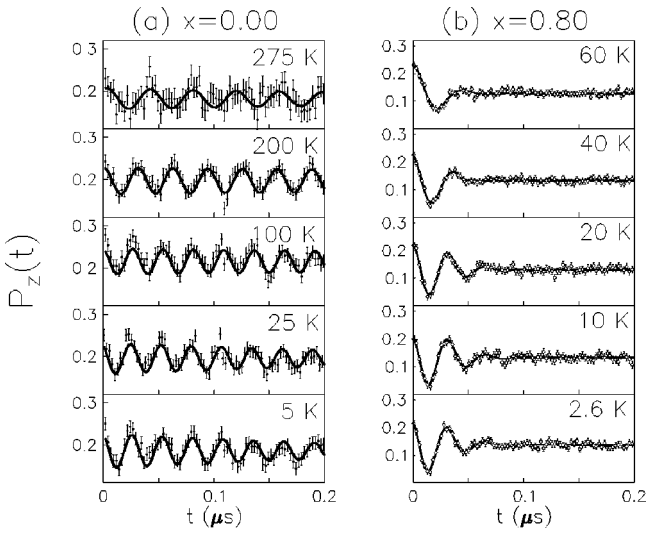

FIG. 1. Time dependence of the muon decay asymmetry for $La_{2-x}Sr_xNiO_{4+\delta}$ (see Table I). We display (a) the short time behavior for $x = 0.00$, showing fast, relatively long-lived coherent precession and (b) the short time behavior for $x = 0.80$, showing damped coherent precession. The smaller error bars in (b) result from higher counting statistics.

results in an apparent missing fraction in the data below T_M since fast oscillations and/or fast relaxations will be averaged to zero, i.e., $P_z(t) = G_\parallel(t)$. By contrast, for each of our samples the fast oscillations were resolvable at PSI. This is illustrated in Fig. 1. The frequencies of the oscillations are obtained by fitting Eq. (3.2) to the data in the relevant time range. The following phenomenological functions are assumed in order to accurately model the zero-frequency component and the rapid decay of the oscillations:

$$G_\parallel(t) = a\exp(-\lambda_\parallel t), \tag{4.1}$$

$$G_\perp(t) = b\exp(-\lambda_\perp t). \tag{4.2}$$

A constant nonrelaxing term is also added to model the polarization of muons which miss the sample and stop in the silver backing plate. In all the samples measured at PSI we observed clear single frequency oscillations in zero applied field (see Fig. 1), except in the almost stoichiometric sample ($x = 0.00$, see Table I) where we find *two* oscillatory signals (see also Ref. 32). The second *low* frequency signal can also be seen in the ISIS data for temperature above $\approx$100 K. In Sec. IV D below we discuss how we can associate the two frequencies with particular muon sites within the crystal.

The magnetic transition temperature T_M for each of the samples is listed in Table I. This quantity is estimated by studying the temperature dependence of the zero-field initial amplitudes using a coarse binning of the data. We define T_M as the temperature corresponding to 0.5Δ and the lower and upper bounds for T_M as the temperatures corresponding to 0.2Δ and 0.8Δ, where Δ is the change in the initial amplitude between the high and low temperatures. Figure 2 shows a typical result.

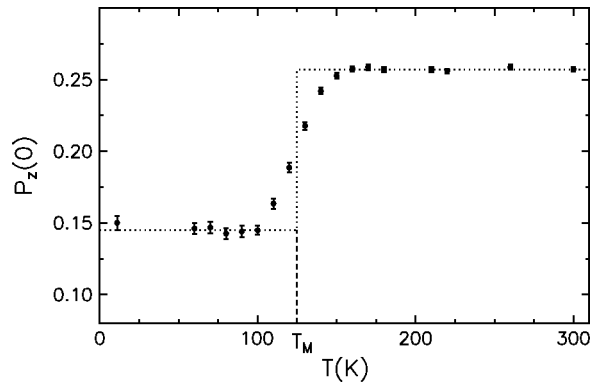

FIG. 2. Initial muon decay asymmetry for the $x=0.20$, $\delta=0.052(3)$ sample (see Table I), as measured at ISIS. The magnetic transition temperature T_M is indicated (see text).

A. Magnetic order in samples

As mentioned above, in all samples coherent precession in zero applied field is observed below T_M. This implies that at a particular temperature below T_M the muon senses an internal magnetic field of essentially constant magnitude which is either static or quasistatic on a time scale of the order of microseconds. The Larmor frequency $\nu_\mu(x,T)$ of the oscillations is proportional to the magnetic field $B_\mu(x,T)$ at the muon site, $\nu_\mu=\gamma_\mu B_\mu/(2\pi)$, and hence to the staggered magnetization $M^{\perp}(x,T)$. We attribute the source of the internal field to the ordered nickel moments in the vicinity of the muon.

Some authors have suggested on the basis of magnetic susceptibility measurements that $La_{2-x}Sr_xNiO_{4+\delta}$ might have a spin glass ground state.[21,22] In a spin glass the muons would see a very broad distribution of local magnetic fields, leading to a noncoherent precession.[23] Such a behavior is not found in our experiments. We conclude that our samples do not show spin-glass behavior but cannot rule out the possibility that there is a small fraction of each sample ($<5\%$) that might exhibit spin glass behavior which dominates the magnetic susceptibility, but because of its low volume fraction is unobservable in μSR.

Figure 3 shows the temperature dependence of $\nu_\mu(x,T)$ for several different dopings. A fit of our data to the function

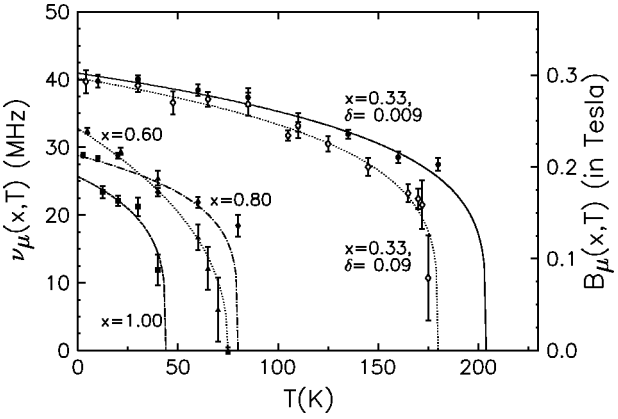

FIG. 3. Temperature dependence of muon precession frequencies in $La_{2-x}Sr_xNiO_{4+\delta}$ for various x values. The lines are the fitting functions $\nu_\mu(x,T)=\nu_\mu(x,0\text{ K})[1-T/T_M(x)]^{\beta(x)}$.

$\nu_\mu(x,T)=\nu_\mu(x,0\text{ K})\{1-[T/T_M(x)]\}^{\beta(x)}$ using the values of T_M listed in Table I yields a value of $\beta(x)$ of 0.22 ± 0.02 and 0.22 ± 0.01 for the $x=0.33$ samples ($\delta=0.009$ and 0.08, respectively), 0.22 ± 0.02 for $x=0.80$, 0.24 ± 0.04 for $x=1.0$ and 0.43 ± 0.04 for $x=0.60$. Our functional form of $\nu_\mu(x,T)$ gives a good description of the data over the complete temperature range. Theoretical values of the exponent β for 3D Heisenberg, *XY* and Ising systems are 0.38, 0.33, and 0.31, respectively,[24] while the value for a 2D *XY* model[25] is 0.23, consistent with values found in other 2D magnetic systems.[26,27] The values of β for most of our samples are close to the theoretical value for 2D *XY* systems, and are consistent with the two-dimensional character of these materials even though the functional form used is normally only expected to be applicable to a small range below the temperature of the phase transition. The $x=0.60$ sample shows a qualitative difference of the temperature dependence from the other samples. The reason for this difference in behavior for this composition is not clear at present.

It is notable that magnetic order persists in these samples to much higher hole concentrations than in $La_{2-x}Sr_xCuO_{4+\delta}$.[28] This is consistent with the suggestion[27] that mobile holes are more effective in destroying the exchange interaction giving rise to magnetic order than less mobile holes.[4] The holes in $La_{2-x}Sr_xNiO_{4+\delta}$ have a greater $3d$ character compared to those in $La_{2-x}Sr_xCuO_{4+\delta}$ and are therefore expected to be less mobile. The existence of less mobile holes is also consistent with the much higher Sr doping concentration needed to induce metallic conductivity in $La_{2-x}Sr_xNiO_{4+\delta}$ (Ref. 4 and below).

Figure 4(a) shows the doping dependence of the Larmor frequency $\nu_\mu(x,T=0\text{ K})$ extrapolated to $T=0$ K. The data set (excluding the $x=0.33$ points) is fitted to the phenomenological function[27] $\nu_\mu(x,T=0\text{ K})=\nu_\mu(x=0,T=0\text{ K})\times(1-x/x_c)^n$, and as best fit we get $x_c=1.02$ and $n=0.113$. Reasonable fits can also be obtained for values $1.02\leqslant x_c<\sim1.08$, see Fig. 4(a). x_c can be interpreted as the doping level where the magnetic order is lost and a phase transition to a metallic state occurs. Our estimate of x_c is consistent with the value $x_c\approx1$ determined by an NMR study.[29] Note that the values of ν_μ in our less heavily doped samples are close to the high frequency precession in the undoped material [Fig. 1(a)]. This implies that the *average* local field detected by the muon is similar in the doped and the parent material, a result which was also found[30] in lightly doped $La_{2-x}Sr_xCuO_4$. However, there is a peak in the frequency in $x=0.33$. Such behavior is qualitatively consistent with a higher localization of the holes at this concentration alluded to in the Introduction. The model presented in Ref. 27 to explain the anomalous low-temperature rise in the local magnetic field seen by the muon in $La_{2-x}Sr_xCuO_4$, suggests that the effective size of the magnetic domains determines both the local staggered magnetization and the transition temperature T_M. In particular, both these quantities decrease with decreasing domain size. Within the context of this model, we can visualize that in $La_{2-x}Sr_xNiO_4$ samples where $x\neq0.33$, the holes act similar to ''flowing rivers'' of charge which form walls in the Ni-O planes separating undoped antiferromagnetic (AFM) domains. However, at $x=0.33$, the holes are more localized and this leads to larger effective domain sizes and hence a corresponding increase in the local stag-

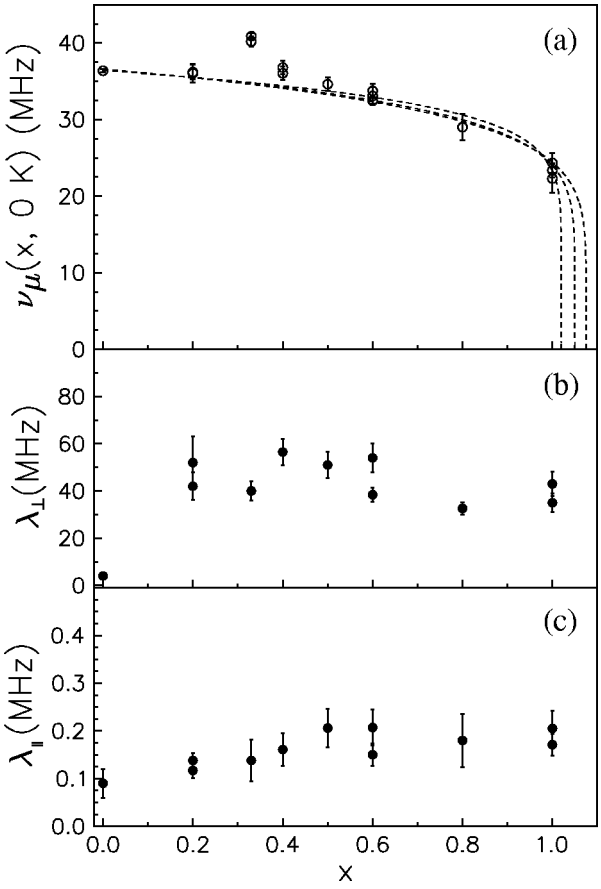

FIG. 4. (a) Low-temperature Larmor frequency vs doping level x (see text). Note the peak at $x=0.33$. We also display a range of reasonable fits to the phenomenological function $\nu_\mu(x,T=0\ \mathrm{K}) = \nu_\mu(x=0,T=0\ \mathrm{K})\times(1-x/x_c)^n$, with ($x_c=1.02$, $n=0.113$), ($x_c=1.05$, $n=0.138$) and ($x_c=1.075$, $n=0.152$). (b) Low-temperature damping rate $\lambda_\perp$ as a function of x. (c) Low-temperature damping rate $\lambda_\parallel$ as a function of x.

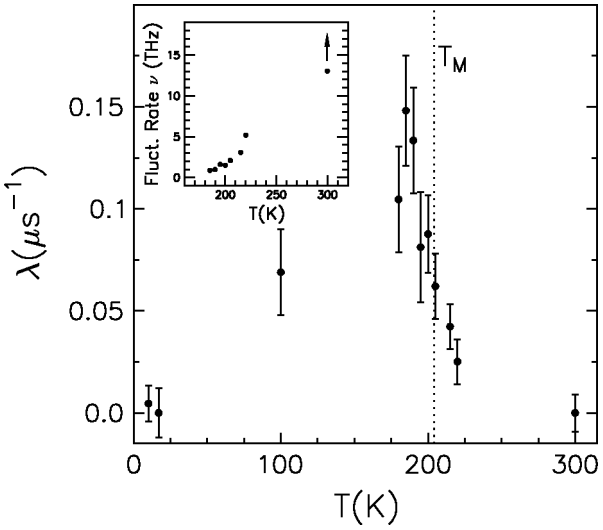

FIG. 5. Exponential relaxation rate λ and spin fluctuation rate ν (inset) for the $La_{1.67}Sr_{0.33}NiO_{4.010}$ sample in zero magnetic field. The fluctuation rate is calculated in the fast fluctuation limit (see Sec. IV B).

gered magnetization. Note that this model also predicts the existence of a peak in T_M, an issue that we will return to in Sec. IV C.

B. Static and dynamic nature of the nickel spins

We now discuss the damping rates $\lambda_\perp$ of the oscillating signals as well as $\lambda_\parallel$ [see Eqs. (4.2) and (4.1), respectively]. The implications of these results will be discussed in the context of our previous μSR study[19] of polycrystalline $La_{2-x}Sr_xNiO_4$ as well as to neutron measurements in nickelates with lower hole doping levels[8,9,11] (these show evidence for stripe spin and hole order, a phase which is quite different from the Néel state of the parent material[31]). The observation that $\lambda_\perp \gg \lambda_\parallel$ for all x, as shown in Figs. 4(b) and 4(c), indicates that the relaxation of the oscillations is dominated by the *static* distribution of the neighboring Ni spins. Nevertheless, some *dynamic* broadening, i.e., fluctuations of the Ni spins, is undoubtedly present since $\lambda_\parallel$ is nonzero.

The large values of $\lambda_\perp$ indicate that there is a significant inhomogeneity in the local spin structure around the muon. This broadening ranges from $\lambda_\perp(x,T\to 0\ \mathrm{K})/[2\pi\nu_\mu(x,T\to 0\ \mathrm{K})]=1.8$ % in the $x=0.00$, $\delta=0.009$ sample to $\approx 28.2\%$ in the $x=1.00$, $\delta=0.00$ sample. Such inhomogeneities might arise from the formation of stripe phases; however, the muon is not sensitive to the details of this local spin structure, as evidenced by the nearly constant $\lambda_\perp$ for $x\neq 0$. (No clear correlation is seen between stripe formation at the ''special'' doping value of $x=0.33$ and $\lambda_\perp$.) The spin fluctuation rates are significantly less than $\gamma_\mu B_\mu$ since coherent precession is observed, implying that the correlation time of the nickel spins is longer than 10^{-8} s at low temperatures. In this context it is interesting to note that in a sample with $x=0.2$ (δ not measured) the magnetic correlation time for correlated regions (stripes) was found by neutron scattering[12] to be longer than $\sim 10^{-11}$ s at 2 K and of the order of $\sim 10^{-12}$ s at 80 K.

The source of the muon relaxation for $T \gg T_M$ was attributed earlier to *nuclear* dipolar fields.[19] In our present study we have confirmed this for a number of samples by the observation that a weak longitudinal field of ≈ 10 mT is sufficient to quench the relaxation, i.e., $P_z(t)$ is almost constant. This was checked in the $x=0.25$, $x=0.33$, $x=0.40$, $x=0.50$, and $x=1.00$ samples. The nuclei responsible for the relaxation are likely to be ^{139}La, the most abundant species with nonzero nuclear spin (the natural abundances are ^{138}La 0.089% and ^{139}La 99.911%, the nuclear spin of ^{139}La is 7/2). In this high-temperature range the fluctuation rate of the nickel moments is much higher than the Larmor frequency of the muon; hence, the muon polarization does not relax (motionally narrowed limit).

In the fast fluctuation limit in zero applied field the exponential relaxation rate above the magnetic transition is given by[23,33] $\lambda = 2\gamma_\mu^2 B_{\mathrm{rms}}^2 \tau$. Here τ is the correlation time of the internal field and B_{rms} is the rms internal magnetic field at the muon site, assumed to be of the order of the average magnetic field sensed by the muons at the lowest temperatures. We estimated λ from a short-time exponential fit to $P_z(t)$. This fit is valid since the Gaussian relaxation (see above) will be dominant only on a longer time scale.[34] A representative plot of the temperature dependence obtained from the relaxation rates, is displayed in Fig. 5. λ is too small to be

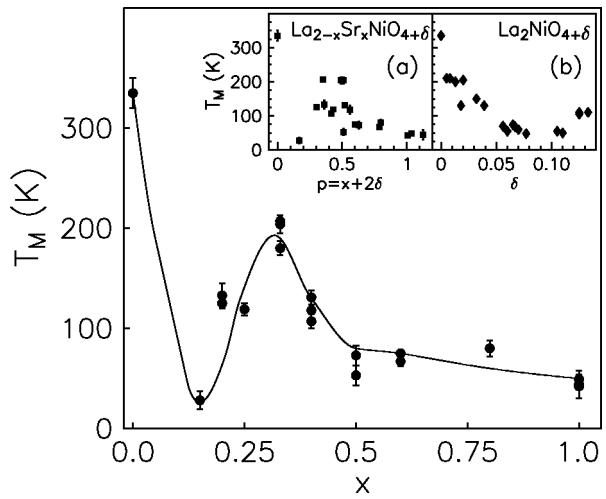

FIG. 6. Phase diagram for $La_{2-x}Sr_xNiO_{4+\delta}$. Multiple entries for the same x value are associated with different δ values (see Table I). The solid line is a guide to the eye. Inset (a) shows the same data set, plotted as a function of $p=x+2\delta$. Clearly p is not the appropriate parameter for the characterization of the magnetic transition temperature. Inset (b) shows the dependence of the magnetic transition temperature on the oxygen doping in $La_2NiO_{4+\delta}$ (taken from references cited in the text). A similar sensitivity of the transition temperature to oxygen doping is not apparent in the strontium doped compounds that we have studied (see Sec. IV C).

measurable at 300 K so that using $\lambda \ll 0.01\ \mu s^{-1}$ we estimate that the correlation time of the Ni spins is smaller than 10^{-13} s (shorter than previously[19] reported). We also note that the muon is not diffusing very rapidly on a microsecond time scale since a coherent precession is observed by μSR in stoichiometric La_2NiO_4 up to 335 K.

C. Phase diagram of the magnetic transition

We now discuss the dependence of T_M on the strontium doping concentration. The measurements are summarized in Fig. 6. The different T_M values for a given x are associated with different values of δ, e.g., the three values of T_M represented for $x=0.40$ correspond to $\delta=0.08$, $\delta=0.06$, and $\delta=0.008$. The transition temperatures for a particular x are, however, very close to each other even though δ is different in each case (see Table I). Contrast this behavior with the $x=0$ material [see inset (b) in Fig. 6, data taken from Refs. 7,16,35–37], where a drastic initial drop in the magnetic transition temperature is seen with increasing δ. We find that T_M first drops with increasing x, reaches a minimum at $x\sim 0.15$, and then rises again to a maximum of ≈ 205 K for $x=0.33$. For larger x the transition temperature again drops, falling to a value of about 45 K at our highest doping levels (Fig. 6).

In Ref. 19 we speculated that $p=x+2\delta$ might be the relevant parameter for controlling the magnetic transition temperature, following a suggestion based on neutron measurements.[8] Our current study, making use of many more samples, demonstrates that this appears to be incorrect for $La_{2-x}Sr_xNiO_{4+\delta}$ where $x\neq 0$ (see Table I). This is particularly obvious from inset (a) in Fig. 6 where there are a number of very different T_M values for a particular value of p. The interstitial accommodation of oxygen requires a local lattice distortion[37] while quite different structural consequences result from Sr substitution.[38] Both these structural effects are likely to have significant, but dissimilar, effects on the magnetic properties even when the nominal hole concentration is identical.

Based on neutron scattering experiments, it has been suggested[13] that spin stripe ordering is driven by charge ordering. The $x=0.33$ doping has attracted much attention because it demonstrates pronounced charge ordering (at 239 K).[13,17] We believe that the loss of hole mobility is responsible for the pronounced increase in T_M (Fig. 6) at this doping level. In view of our earlier discussion (Sec. IV A) regarding the effects of the magnetic domain size on $\nu_\mu(x, T=0\ \mathrm{K})$, a peak in T_M is also expected and indeed observed at this special concentration. For $x=0.5$, anomalies in bulk properties, e.g., resistivity,[17] have previously been observed at higher temperatures (~ 340 K), but the features were much broader and weaker than those for $x=0.33$. We find no evidence of another peak in T_M at this hole doping level.

D. Muon site

In agreement with Ref. 32 we find two distinct values of ν_μ in our $x=0.00$ sample, which can be attributed to two muon sites. There is no indication of a second muon site for any of the Sr doped samples. In order to arrive at possible muon sites in $La_{2-x}Sr_xNiO_{4+\delta}$, we have performed dipole field calculations, analogous to those described elsewhere.[39,40] The local magnetic field $\mathbf{B}_\mu(\mathbf{r}_\mu)$ sensed by the muon is given by the sum of the dipolar field $\mathbf{B}_{\mathrm{dip}}(\mathbf{r}_\mu)$, due to Ni moments and the hyperfine field $\mathbf{B}_{\mathrm{hf}}(\mathbf{r}_\mu)$, due to any nonzero electron spin density at the muon site. Although we lack knowledge of the hyperfine coupling constant it is assumed to be small, as in the case[39] of La_2CuO_4 and other magnetic oxides. With this assumption the magnetic field at the muon site can be calculated as a sum of dipolar contributions

$$\mathbf{B}_\mu(\mathbf{r}_\mu)=\sum_i \frac{3(\boldsymbol{\mu}_i\cdot\mathbf{n}_i)\mathbf{n}_i-\boldsymbol{\mu}_i}{|\mathbf{r}_\mu-\mathbf{r}_i|^3}, \tag{4.3}$$

where $\mathbf{r}_\mu$ is the position of the muon, $\boldsymbol{\mu}_i$ is the effective magnetic moment of the ith nickel ion, and $\mathbf{n}_i$ is the unit vector from the muon to the nickel ion at site $\mathbf{r}_i$. The magnetic moment $\boldsymbol{\mu}_i$ of La_2NiO_4 has been measured by neutron diffraction.[35,36] The values obtained in the two studies were 0.75 and $0.85\mu_B$, respectively. In our calculations we assumed the mean of those values, i.e., $|\boldsymbol{\mu}_i|=0.80\mu_B$. From Ref. 35 we have taken the lattice parameters (neglecting the small differences in the two lattice constants a and b) of $a=b=3.87$ Å, $c=12.63$ Å and the spin structure as shown in Fig. 7(a). The sum in Eq. (4.3) was evaluated numerically by taking into account nickel spins within a radius of $15a$ about $\mathbf{r}_\mu$.

In the Ni-O plane the field distribution is rather flat in the center of the plane but changes rapidly near the nickel sites (where the field diverges) and the oxygen sites (where the field is zero); see Fig. 7(b). As one would expect, outside this plane the field is much smaller, and becomes smallest in the $z/c=1/4$ plane (where the maximum value is $|\mathbf{B}|=41$ mT).

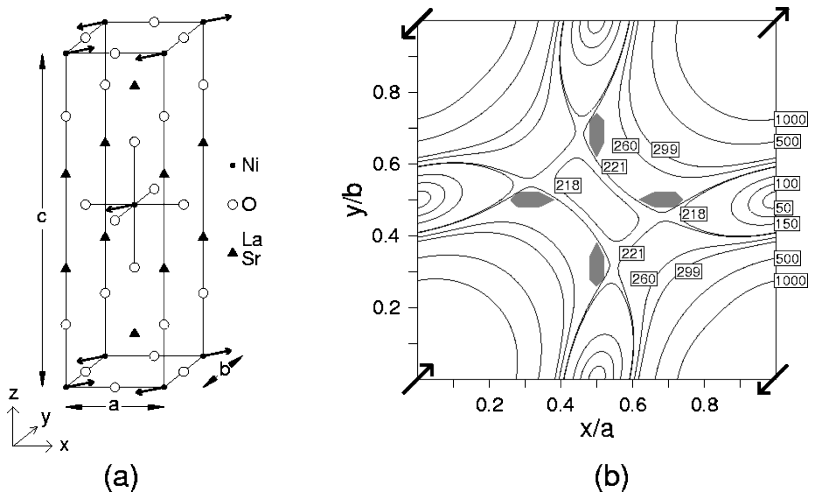

FIG. 7. (a) Structure (Ref. 35) of La_2NiO_4. The nickel moments, symbolized by arrows, point along the $\langle 110 \rangle$ directions. The lattice parameters (Ref. 35) are $a=b=3.87$ Å, $c=12.63$ Å. (b) Contour plot of the dipole field in the $z/c=0$ plane. The nickel moments are symbolized by arrows at the corners of the square. The shaded region corresponds to the computed muon positions. The magnetic field is given in mT.

We selected sites which are within 15% of 260 mT; this field value corresponds to the high precession frequency observed in our nearly stochiometric sample, $x=0.0$, $\delta=0.009$. The 15% tolerance reflects the uncertainty in the magnetic moment from the neutron measurements. We find that the muon distance to the Ni-O plane should be smaller than 1.3 Å. Restrictions can be imposed because crystallographically equivalent sites in the unit cell do not experience the same magnetic field (the field symmetry is reduced due to the spin structure), i.e., in general $|\mathbf{B}(x,y,z)| \neq |\mathbf{B}(x,b-y,z)|$. Assuming that the field distribution is less than 5% of the mean value (given in Sec. IV B), the two possible sites in the Ni-O plane are (1) $x/a=0.4$, $y/b=0$ (and equivalent sites) and (2) those regions in Fig. 7(b) which are shaded. For case (1) the distance to the oxygen (at $x/a=0.5$, $y/b=0$) would be rather small compared to typical O-H bonding lengths of 1 Å. We conclude that within the magnetic dipole approximation, position (2) is the most likely muon site in the Ni-O plane. An analogous treatment for the second lower precession frequency in La_2NiO_4 leads to a range of possible second muon sites, some of which are consistent with the ones proposed for La_2CuO_4.[39]

V. CONCLUSIONS

In conclusion, we have studied magnetic order in $La_{2-x}Sr_xNiO_{4+\delta}$ for a large number of samples where $0 \leqslant x \leqslant 1$ and demonstrated that local magnetic order exists in all samples below an x-dependent transition temperature T_M. This enabled us to probe the temperature dependence of the short-range order parameter in the samples and make estimates of the correlation times below and above the transition temperature. We have extended the information on magnetic transition temperatures to doping values other than those previously reported, and conclude that, in contrast to previous speculations,[8,19] the appropriate parameter for controlling the magnetic transition temperature for nonzero x is not $p=x+2\delta$, but x itself. In light of the coherent precessions obtained in the experiments, the previous speculation[21,22] that the ground state for these materials at higher strontium doping levels is a spin glass needs further exploration. We find evidence for an enhancement in T_M and the zero temperature staggered magnetization associated with doping at $x=\frac{1}{3}$ which may be connected with enhanced hole ordering.

ACKNOWLEDGMENTS

We would like to thank S.P. Cottrell at ISIS and U. Zimmermann and A. Amato at PSI for valuable experimental assistance. We would also like to thank S.F.J. Cox and M. Greven for helpful discussions and our collaborators from TRIUMF and Oxford who took part in our earlier preliminary study (Ref. 19). This work is partially supported by EPSRC (UK) and NSERC (Canada). T.J. would like to thank the European Commission for financial support in the framework of the TMR program. J.E.M. would like to thank the donors of the Petroleum Research Fund, administered by the American Chemical Society, for financial support.

*Electronic address: t.jestadt@physics.ox.ac.uk

†Present address: Department of Physics, Lehigh University, 16 Memorial Drive East, Bethlehem, PA 18015.

[1] T. R. Thurston, R. J. Birgeneau, M. A. Kastner, N. W. Preyer, G. Shirane, Y. Fujii, K. Yamada, Y. Endoh, K. Kakurai, M. Matsuda, Y. Hidaka, and T. Murakami, Phys. Rev. B **40**, 4585 (1989).

[2] S.-W. Cheong, G. Aeppli, T. E. Mason, H. Mook, S. M. Hayden, P. C. Canfield, Z. Fisk, K. N. Clausen, and J. L. Martinez, Phys. Rev. Lett. **67**, 1791 (1991).

[3] J. G. Bednorz and K. A. Müller, Z. Phys. B **64**, 189 (1986).

[4] R. J. Cava, B. Batlogg, T. T. Palstra, J. J. Krajewski, W. F. Peck, A. P. Ramirez, and L. W. Rupp, Phys. Rev. B **43**, 1229 (1991), and references therein.

[5] G. Tavizón, E. Orgaz, and R. Escudero, Physica C **185-189**, 517 (1991).

[6] C. H. Chen, S.-W. Cheong, and A. S. Cooper, Phys. Rev. Lett. **71**, 2461 (1993).
[7] K. Yamada, T. Omata, K. Nakajima, and Y. Endoh, Physica C **221**, 335 (1994).
[8] V. Sachan, D. J. Buttrey, J. M. Tranquada, J. E. Lorenzo, and G. Shirane, Phys. Rev. B **51**, 12 742 (1995).
[9] J. M. Tranquada, D. J. Buttrey, V. Sachan, and J. E. Lorenzo, Phys. Rev. Lett. **73**, 1003 (1994).
[10] J. M. Tranquada, Y. Kong, J. E. Lorenzo, D. J. Buttrey, D. E. Rice, and V. Sachan, Phys. Rev. B **50**, 6340 (1994).
[11] J. M. Tranquada, J. E. Lorenzo, D. J. Buttrey, and V. Sachan, Phys. Rev. B **52**, 3581 (1995).
[12] S. M. Hayden, G. H. Lander, J. Zarestky, P. J. Brown, C. Stassis, P. Metcalf, and J. M. Honig, Phys. Rev. Lett. **68**, 1061 (1992).
[13] J. M. Tranquada, D. J. Buttrey, and V. Sachan, Phys. Rev. B **54**, 12 318 (1996).
[14] J. M. Tranquada, P. Wochner, A. R. Moodenbaugh, and D. J. Buttrey, Phys. Rev. B **55**, R6113 (1997).
[15] J. M. Tranquada, P. Wochner, and D. J. Buttrey, Phys. Rev. Lett. **79**, 2133 (1997).
[16] K. Nakajima, Y. Endoh, S. Hosoya, J. Wada, D. Welz, H. M. Mayer, H. A. Graf, and M. Steiner, J. Phys. Soc. Jpn. **66**, 809 (1997).
[17] S.-W. Cheong, H. Y. Hwang, C. H. Chen, B. Batlogg, L. W. Rupp, Jr., and S. A. Carter, Phys. Rev. B **49**, 7088 (1994).
[18] S.-H. Lee and S.-W. Cheong, Phys. Rev. Lett. **79**, 2514 (1997).
[19] K. H. Chow, P. A. Pattenden, S. J. Blundell, W. Hayes, F. L. Pratt, Th. Jestädt, M. A. Green, J. E. Millburn, M. J. Rosseinsky, B. Hitti, S. R. Dunsiger, R. F. Kiefl, C. Chen, and A. J. S. Chowdhury, Phys. Rev. B **53**, R14 725 (1996).
[20] J. H. Brewer, *Encyclopedia of Applied Physics* (VCH Publishers, New York, 1994), Vol. 11, pp. 23–53; A. Schenck, *Muon Spin Rotation: Principles and Applications in Solid State Physics* (Hilger, London, 1985); S. F. J. Cox, J. Phys. C **20**, 3187 (1987); A. Schenck and F. N. Gygax, *Handbook of Magnetic Materials* (North-Holland, Amsterdam, 1995), Vol. 9, pp. 57–302; P. Dalmas de Réotier and A. Yaouanc, J. Phys.: Condens. Matter **9**, 9113 (1997).
[21] G. H. Lander, P. J. Brown, C. Stassis, P. Gopalan, J. Spalek, and G. Honig, Phys. Rev. B **43**, 448 (1991).
[22] Th. Strangfeld, K. Westerholt, and H. Bach, Physica C **183**, 1 (1991).
[23] Y. J. Uemura, T. Yamazaki, D. R. Harshman, M. Senba, and E. J. Ansaldo, Phys. Rev. B **31**, 546 (1985).
[24] Sheng-Keng Ma, *Modern Theory of Critical Phenomena* (Benjamin, New York, 1976).
[25] S. T. Bramwell and P. C. W. Holdsworth, J. Phys.: Condens. Matter **5**, L53 (1993).
[26] L. J. de Jongh and A. R. Miedema, Adv. Phys. **23**, 1 (1974).
[27] F. Borsa, P. Carretta, J. H. Cho, F. C. Chou, Q. Hu, D. C. Johnston, A. Lascialfari, D. R. Torgeson, R. J. Gooding, N. M. Salem, and K. J. E. Vos, Phys. Rev. B **52**, 7334 (1995).
[28] E. Dagotto, Rev. Mod. Phys. **66**, 763 (1994).
[29] Y. Furukawa and S. Wada, J. Phys.: Condens. Matter **6**, 852 (1996).
[30] D. R. Harshman, G. Aeppli, G. P. Espinosa, A. S. Cooper, J. P. Remeika, E. J. Ansaldo, T. M. Riseman, D. L. Williams, D. R. Noakes, B. Ellman, and T. F. Rosenbaum, Phys. Rev. B **38**, 852 (1988).
[31] G. Aeppli and D. J. Buttrey, Phys. Rev. Lett. **61**, 203 (1988).
[32] B. Martínez, X. Obradors, E. J. Ansaldo, C. Niedermayer, D. R. Noakes, M. J. Sayagués, M. Vallet, and J. González-Calbet, J. Magn. Magn. Mater. **104-107**, 941 (1992).
[33] A. Keren, Phys. Rev. B **50**, 10 039 (1994).
[34] In addition, we experimentally confirmed this in some of our samples by applying a longitudinal field of between 5 and 10 mT. The Gaussian contribution disappears but the exponential part remains the same within the error bars.
[35] T. Fretoft, D. J. Buttrey, G. Aeppli, D. Vaknin, and G. Shirane, Phys. Rev. B **44**, 5046 (1991).
[36] J. M. Tranquada, D. J. Buttrey, and D. E. Rice, Phys. Rev. Lett. **70**, 445 (1993).
[37] P. Gopalan, M. W. McElfresh, Z. Kakol, J. Spalek, and J. M. Honig, Phys. Rev. B **45**, 249 (1992).
[38] P. J. Heaney, A. Mehta, G. Sarosi, V. E. Lamberti, and A. Navrotsky, Phys. Rev. B **57**, 10 370 (1998).
[39] L. P. Le, G. M. Luke, B. J. Sternlieb, Y. J. Uemura, J. H. Brewer, T. M. Riseman, D. C. Johnston, L. L. Miller, Y. Hidaka, and H. Murakami, Hyperfine Interact. **63**, 279 (1990).
[40] K. H. Chow, Th. Jestädt, S. J. Blundell, S. R. Dunsiger, W. Hayes, B. Hitti, M. A. Green, R. F. Kiefl, J. E. Millburn, P. A. Pattenden, F. L. Pratt, and M. J. Rosseinsky, Hyperfine Interact. **104**, 55 (1997).